

ISR-BOM/PJB et al./rh

7 January 1977

CERN LIBRARIES, GENEVA



CM-P00072215

ISR PERFORMANCE REPORT

Run 776 - 18 November 1976 - 26 GeV/c - Rings 1 and 2

Run 791 - 13 December 1976 - 26 GeV/c - Physics set-up and run

Run 794 - 20 December 1976 - 26 GeV/c - Physics run and luminosity

First running-in tests of the Il superconducting solenoid

1. Conclusions

The solenoid has been successfully used for physics.

The coupling excited by the solenoid is in exact agreement with the predicted value. As expected, the working line is unperturbed and the closed orbit behaves as foreseen except for a small discrepancy in the vertical orbit. The resonance excitation is negligible compared to the beam-beam effect for high orders ( $>5$ ) which is fortunate for the background production. For the 5th order resonances, the excitation is about 5 times that of the basic ISR and comparable to the beam-beam excitation but it is not troublesome. Lower order resonances were not studied.

It appears that it is best to correct the horizontal orbit perturbation arising from the solenoid with COCO and to keep a set of special closed orbit files for the solenoid, rather than making a local correction with the adjacent CR windings. For the vertical orbit, the theoretical settings for the compensator magnets appear to be 1.25 % of  $I_{\max}$  too high. The source of this error is, for the moment, a mystery. The same error, however, may also be the cause of the residual distortions observed with the Il luminosity bumps with the low- $\beta$  on<sup>2</sup>). The optimized compensator settings are:

Compensator settings for low- $\beta$  off

$$\begin{array}{lcl} C1 = 57.53 \% & \} & C2 = 57.61 \% \\ C3 = 72.19 \% & \} \text{ Ring 1} & C4 = 72.15 \% \} \text{ Ring 2} \end{array}$$

(values should be set on upward branch of hysteresis curve, i.e. 0 % to +100 % to 0 % to set value).

A further mystery, which is not directly related to the solenoid, is the source of the strong coupling excitation in the basic ISR. This

coupling is of nearly the same amplitude in the two rings ( $|C| \simeq 10^{-2}$ ) but of opposite sign and is roughly three times the coupling due to the solenoid. If random magnet tilts were to be the source, the r.m.s. tilt would have to be 1 mrad, which is surely not the case. The alternative is an integrated skew gradient of 0.33 T, which again cannot be explained by alignment errors. Some difficulties in measuring the Q-values on 8C type WL's for acceleration have recently been observed which is not surprising since the Q-meter cannot measure when  $(Q_h - Q_v)$  is less than  $|C|_{ISR}$  which is 0.01.

In the physics run 791, only the basic ISR machine coupling was compensated. With the existing skew quadrupole scheme, the compensation of the solenoid's coupling entails large currents and the excitation of median plane tilts. Since the run was a success, it is proposed that this procedure be continued until the new skew quadrupole scheme is installed.

The solenoid still has to be tested with the low- $\beta$  scheme.

## 2. Set-up conditions for the MD Run 776

Both rings were set up for the ELSA working line with the low- $\beta$ , the SFM, the solenoid and all other experimental magnets off. The B-pulse was changed to move the injection orbit to  $\bar{x} = -36$  mm in order to simplify the set-up for the low- $\beta$  test which followed. The tune spreads were reduced ( $Q'_h = Q'_v \simeq 1$ ) in ring 1 for coupling measurements. Closed orbit, working line, coupling, resonance excitation and pulse profile measurements were made. The solenoid was then switched on and set to 2170 A before repeating the same series of measurements.

The field of the solenoid was opposed to the beam direction in ring 1, i.e. the South pole faced I2. For this field configuration, the interaction diamond is above the median plane (see Fig. 1 and Appendix B). The standard ISR convention that positive currents give an upward kick has been adopted for the compensators. Hence, for the solenoid field defined above, the compensator currents are positive in both rings. The sign attributed to the solenoid current on the SRC display panel was arbitrarily chosen as negative but disconcertingly this changed to positive between runs 776 and 779 (without the field being changed).

Just prior to this run, the upstream compensator in ring 2 was found to be displaced towards the intersection by 11 cm from its nominal position. The tracking program for the solenoid was re-run and the compensators were adjusted differently in the two rings to account for this.

3. Set-up and running conditions for the Physics Run 791

Both rings were set up for the ELSA working line with the low- $\beta$  off but with the SFM, the solenoid and the I2 and I7 experimental magnets on. A part of the set-up was devoted to optimizing the vertical closed orbit. The upstream compensator in ring 2, which had been misaligned by 11 cm towards the intersection in the earlier run 776, had been re-aligned and the current settings reverted to the standard values in both rings. The basic ISR coupling was compensated in both rings by setting  $Q_2 = -4.6\%$ . The solenoid's coupling was left uncompensated but this causes no problems. Although it is theoretically possible to compensate the solenoid, it requires large currents in the skew quadrupoles and introduces median plane tilts especially outside the intersection regions.

4. Effect of the solenoid on closed orbits

4.1 Measurements from Run 776

The vertical closed orbit measurements made in ring 2 during the first run 776 are summarized in Table 1. The compensators for correcting the vertical orbit were set to values calculated with a tracking program using a field plot for the solenoid supplied by S. Pordes of EP Division. As can be seen, at  $\bar{x} = +40$  mm there is an additional distortion of 6.6 mm which diminished to 1.2 mm peak-to-peak at injection.

Radial position $\bar{x} =$	Solenoid off			Solenoid on		
		-35.5	0.7	39.9	-34.2	-1.9
Vertical pk-to-pk =	7.4	7.8	10.7	8.6	9.7	17.3
Vertical r.m.s. =	1.6	1.7	2.7	2.0	2.4	4.8

TABLE 1

Comparison of the vertical closed orbits in ring 2  
with and without the solenoid (Run 776)

This orbit was analysed to find the errors in the compensators. The method of analysis<sup>1)</sup> is based on correlation products between the observed additional distortion arising from the solenoid and its compensators and the calculated distortion patterns of the compensators. The program indicated that:

- the upstream compensator could be +2.4 % of  $I_{\max}$  in error;
- the downstream compensator could be +2.2 % of  $I_{\max}$  in error;
- the two possibilities were of equal probability.

This result suggests that a common error exists and that both compensators were 1.1 to 1.2 % of  $I_{\max}$  too high. As time was limited in the first run and as one ring 2. compensator was in any case misaligned, further investigation of this problem was left until run 791.

The horizontal orbit measurements made in run 776 showed a large distortion at  $\bar{x} = +40$  mm with the solenoid on. This result was surprising and inconsistent with theory (see Appendix B). Once the measurements had been repeated in run 791, it was realized, with some relief, that one of the earlier measurements was completely wrong and that PU832 was consistently giving false readings although at times the values appeared to be reasonable. For these reasons, the horizontal orbit measurements from run 776 are not reproduced here.

#### 4.2 Measurements from Run 791

Table 2 summarizes the closed orbit measurements made during the physics set-up for run 791. An accidental switch-off of the solenoid enabled the reference orbits without the solenoid to be measured. Before measuring the orbits, the compensators were degaussed by following the settings +100 %, -30 %, +10 %, -3 %, +1 %, 0 %. The other three sets of data correspond to the solenoid on and with the compensators set to 1 % of  $I_{\max}$  below the calculated values, the calculated values and finally 1 % of  $I_{\max}$  above the calculated values. These settings were made on the upward branch of the hysteresis curve and after having cycled the compensators 0 %, +100 %, 0 %. Considering the vertical orbit first, it can be seen that the compensators have the best match when set to 1 % of  $I_{\max}$  below the theoretical settings, which agrees with the orbit analysis from the previous run. At injection and centre line,

TABLE 2  
Comparison of closed orbits in ring 2  
with and without the solenoid (Run 791)

Conditions	Radial position $\bar{x}$ (mm)	Horizontal		Vertical	
		pk-to-pk (mm)	r.m.s. (mm)	pk-to-pk (mm)	r.m.s. (mm)
Solenoid off	40.2	-- **	--	5.6	1.0
Compensators	- 2.0	11.5	2.6	4.6	0.8
Degaussed	-38.8	12.4	2.9	4.5	0.8
Solenoid on	40.3	20.4	3.7	7.1	1.3
C2 = 57.86 %	- 1.5	12.7	2.8	4.4	0.8
C4 = 72.40 %	-38.9	13.2	2.9	5.3	0.8
Solenoid on	40.5	20.4	3.7	10.4	2.9
C2 = 58.86 % *	- 2.1	12.5	2.8	6.8	1.6
C4 = 73.40 %	-38.6	13.4	2.9	6.2	1.3
Solenoid on	40.5	20.0	3.7	13.7	4.3
C2 = 59.86 %	- 0.9	12.1	2.9	8.4	2.3
C4 = 74.40 %	-39.1	13.3	2.8	8.4	1.8

\* Theoretical compensator settings calculated with tracking program.

\*\* Printed output of orbit lost and the copy of the television output contains a faulty pickup in the horizontal plane, which invalidates the peak-to-peak and r.m.s. values.

the r.m.s values show no deviations but the peak-to-peak values, however, are less reliable as they depend on only two pickups, which may explain why the orbit is better corrected on the centre line with the solenoid on than with it off while the converse is true at injection. By virtue of the increased sensitivity of the ELSA working line to field errors at the top, the orbit at  $\bar{x} = +40$  mm gives the most reliable guide to the mismatch (see Fig. 2). The r.m.s. values in Fig. 2 give the more reliable indication, so that it appears that the compensators are best matched for 1.25 % of  $I_{\max}$  less than the theoretical settings, which is in exceptionally good agreement with the orbit analysis from the earlier run (1.1 to 1.2 % of  $I_{\max}$ ).

The source of the error in the vertical orbit is somewhat of a mystery, but since the luminosity bumps with low- $\beta$  scheme<sup>2)</sup> on and the solenoid off have a large residual distortion, it appears that the compensators are probably at fault rather than the solenoid.

Horizontally, the orbit is perturbed by an increase of 1 mm peak-to-peak (0.2 mm in r.m.s. value) at the centre line. Unfortunately, the orbit at  $\bar{x} = +40$  mm with the solenoid off only exists as a photograph of the screen display and since the individual readings are not given, the peak-to-peak and r.m.s. values cannot be corrected for a false reading from PU832. The distortion on centre line, however, agrees very well with the expected values (see Appendix B). The perturbation to the horizontal orbit arises mainly from the off-axis path of the beam through the end-plate slots (see Appendix B).

5. Effect of the solenoid on the working line

Theoretically, the focusing effect of the solenoid is given by:

$$\Delta Q_h = 0 ; \quad \Delta Q_v = \frac{\beta_v}{4\pi\ell_s} \left( \frac{B_s \ell_s}{B\rho} \right)^2 = 0.0005 ,$$

for:

solenoid field,  $B_s$  = 1.5 T  
effective field length,  $\ell_s$  = 1.8 m  
 $\beta_v$  at "x" on ELSA = 12.7 m  
 $B\rho = 3.3346$  p for  $p = 26.588$  GeV/c .

The comparison of the working line with and without the solenoid was made in run 776 and is given in Fig. 3. Horizontally, no tune changes can be detected, but vertically a shift of  $\sim 0.002$  exists across most of the aperture. No doubt, the theoretical shift of 0.0005 is present, but the observed shift is almost certainly due to the reproducibility of the working line following some tune shifts made for the resonance excitation experiment which separated the two working line measurements.

Thus, the tune shift associated with the solenoid can almost certainly be neglected.

## 6. Coupling measurements

### 6.1 Summary

The measurements of the modulus of the coupling coefficient  $|C|^{4,5)}$  have been performed with the electronic device built by G. Galbraith and J.P. Gourber. The measurements made in both rings have given the following results:

- i) the amplitude of the machine coupling is now  $\sim 4$  times larger in ring 1 and  $\sim 3$  times larger in ring 2 than in December 1975;
- ii) the machine coupling in ring 2 is  $\sim 20$  % less at the top of the ELSA working line compared to central orbit;
- iii) the calibration of the skew quadrupoles Q2 on the ELSA line, with and without the low- $\beta$  scheme, agrees within 3 to 4 % with the values calculated<sup>6)</sup> from the linear coupling theory<sup>5)</sup>;
- iv) the indirect estimation of the modulus  $|C|$  associated with the detector solenoid in I1 agrees within 8 % with the calculated value<sup>5)</sup>, assuming the phase shift between the solenoid and Q2 is  $76.77^\circ$ ;
- v) the necessary currents in the skew quadrupoles Q1 and Q2 for compensating the coupling of the solenoid are those calculated<sup>5)</sup>, within  $\sim 0.5$  % of the maximum currents.

### 6.2 Results

In run 776, coupling measurements were made in ring 2 on the ELSA working line, without the low- $\beta$  scheme. The machine coupling on central orbit has been found to be

$$\begin{array}{l} \vec{|C}_{R2}| = 0.01096 \\ \text{with} \\ \Delta = Q_h - Q_v = 7.7 \times 10^{-3} \end{array}$$

It was possible to compensate this machine coupling with the skew quadrupoles Q2 (current of  $-4.6$  %). Using the calculated angle for the vector  $\vec{C}$  associated with Q2, the machine coupling  $\vec{C}_{R2}$  and the compensation  $\vec{C}_{Q2}$  are represented in Fig. 4. Figure 4 also gives the results of the Q2 calibration, which agrees within 3.4 % with the theoretical prediction.

The R2 coupling on the ELSA line has been measured at different radial positions (see table below and Fig. 5).

$\bar{x}$ (mm)	$ \vec{C} $ ( $10^{-3}$ )	$Q_h - Q_v$ ( $10^{-3}$ )
-36	10.62	6.57
-20	11.12	7.45
0	10.96	7.7
21.5	9.40	15.9
41.6	9.11	13.9

The detector solenoid in I1 was then switched on and the total coupling was measured for two different distances from the diagonal  $Q_h = Q_v$ :

$$|\vec{C}_{tot}| = 0.0121 \quad \text{with } \Delta = 8.2 \times 10^{-3}$$

and

$$|\vec{C}_{tot}| = 0.0124 \quad \text{with } \Delta = 2.0 \times 10^{-3} .$$

Since the theoretical direction of the vector  $\vec{C}_{sol}$ , due to the solenoid, is known, it is possible to determine the angle  $\psi$  between  $\vec{C}_{sol}$  and  $\vec{C}_{R2}$  and then to calculate the amplitude of  $\vec{C}_{sol}$  using

$$|\vec{C}_{sol}|^2 + 2|\vec{C}_{R2}||\vec{C}_{sol}| \cos \psi + |\vec{C}_{R2}|^2 = |\vec{C}_{tot}|^2 .$$

This gives

$$|\vec{C}_{sol}| = 3.6 \times 10^{-3} .$$

The theoretical value<sup>5)</sup> for the solenoid on ELSA is  $|\vec{C}| = 3.33 \times 10^{-3}$ , and hence the measurement agrees with theory within  $\sim 8\%$ . This also gives an indirect proof that the theoretical angle  $\psi$  is correct. Figure 4 shows how the different coupling vectors are positioned in the complex plane.

Since the measurements were in good agreement with the theoretical predictions, it was decided to directly set the predicted currents of Q1 and Q2 for compensating the solenoid effect, i.e.



$$\left. \begin{array}{l} I_{Q1} = -35.1 \% \\ I_{Q2} = 25.6 \% \end{array} \right\} \text{ Ring 2} \quad \left. \begin{array}{l} = 35.1 \% \\ = -25.6 \% \end{array} \right\} \text{ Ring 1}$$

Adding to these values the necessary current  $I_{Q2} = -4.6 \%$  in order to compensate the R2 machine coupling, the ideal settings for Q1 and Q2 in ring 2 become  $-35.1 \%$  and  $21.0 \%$ . With these currents, the coupling was effectively unmeasurable and the compensation scheme is in agreement with the diagram in Fig. 6.

Some measurements made in the two rings on ELSA with the low- $\beta$  scheme on in run 779 are included here for comparison and completeness. The residual coupling values at the centre line were:

Ring 1	$ \vec{C}_{R1}  = 0.01016$	with $\Delta = 3.5 \times 10^{-3}$
Ring 2	$ \vec{C}_{R2}  = 0.00994$	with $\Delta = 1 \times 10^{-3}$
	$ \vec{C}_{R2}  = 0.00991$	with $\Delta = 4.1 \times 10^{-3}$

Calibrating the skew quadrupoles Q2 in ring 1 (with the low- $\beta$  scheme), the values for 100 % current at 26 GeV are:

$$\begin{array}{l} \text{calculated : } 0.2260 \\ \text{measured : } 0.2176 , \end{array}$$

which gives a difference of 3.7 %. The currents necessary for compensating  $\vec{C}_{R1}$  and  $\vec{C}_{R2}$  have been found to be  $-4.7 \%$  of Q2 and  $-4.6 \%$  of Q2, respectively. The current necessary in ring 2 is the same with and without the low- $\beta$  scheme, since the values of  $|\vec{C}|$  and the efficiencies of Q2 are in the same ratio both with and without the low- $\beta$ . This means that the low- $\beta$  quadrupoles are perfectly aligned and have no effect on the coupling.

## 7. Scrapper scans of single pulses

A series of scrapper scans for a variety of conditions were made on central orbit in ring 1. The main results are summarized in Table 3.

These scans exhibited the now well known, but completely unexplained "hole". In the first group of scans, with the solenoid off, the hole decreases as  $\Delta$  increases or as  $|\vec{C}|$  decreases with the exception of scan No. 2 where the hole appears to be too small. In the second group of

TABLE 3  
Results from scraper scans (Ring 1, 26 GeV/c)

Scan	Conditions	Beam centre (mm)	$ \vec{C}  \times 10^{-3}$	$\Delta$	$h_{\text{eff}}^*$ (mm)	"Hole"width (mm) **	Comments
	<u>Solenoid off</u>						
1	$C_{\text{ISR}}$ compensated	0.024	1.5	0.0077	3.5	0.18	Q2 = -4 %
2	no compensation	0.007	10.9	0.0077	4.4	0.17	Q2 off
3	no compensation	-0.013	10.8	0.0025	6.0	0.34	Q2 off
4	$C_{\text{ISR}}$ compensated	0.005	1.5	0.0025	5.3	0.22	Q2 = -4 %
5	$C_{\text{ISR}}$ compensated	0.003	1.5	-0.0075	3.3	0.15	Q2 = -4 %
6	no compensation	-0.041	10.9	-0.0125	3.4	0.20	Q2 off
7	$C_{\text{ISR}}$ compensated	-0.025	1.5	-0.0125	3.2	0.17	Q2 = -4 %
	<u>Solenoid on</u>						
8	no compensation	0.826	12.1	(0.04)	3.7	0.18	} $\Delta$ estimated from tune shifts
9	no compensation	0.906	12.1	0.0082	6.1	0.31	
10	no compensation	0.859	12.5	0.0020	4.2	0.30	
11	$C_{\text{ISR}}$ compensated	0.871	3.88	0.0020	4.4	0.31	Q2 = -4 %
12	$C_{\text{total}}$ compensated $\approx 0$	0.403	1.3	0.003	4.6	0.23	} Q2 = 21.6 % Q1 = -35.1 %
13	Compensation improved	0.405	not meas- urable	0.003	4.1	0.25	

\*  $h_{\text{eff}}$  is calculated from the scraper scan by subtracting the "hole" and then treating the scan as if there were no coupling. This is almost certainly not a true  $h_{\text{eff}}$  but at present, there is no theory for dealing with the "hole".

\*\* the "hole" appears as a zero current plateau at the pulse centre. No explanations exist for this "hole".

scans, with the solenoid on, the pattern in the results is less clear. Whether the hole can be completely eradicated by a very accurate compensation of the coupling is not known.

The jump of  $\sim 0.8$  mm in the beam centres between the two groups of measurements is probably due to the vertical orbit distortion caused by the compensators (see Section 4).

#### 8. Resonance excitation by the solenoid

These tests were performed in run 776 to get a mainly qualitative idea of the excitation of higher order non-linear resonances by the solenoid. Local bumps were added at each intersection in the same direction as the existing distortion so as to de-couple the two beams vertically. The working line was shifted down the diagonal  $Q_h = Q_v$  until the injection point was at  $Q_h = 8.769$  and  $Q_v = 8.790$  which is just below the resonance  $5Q_h = 44$ . The dump block was then displaced until it just touched the beam halo so that any blow-up arising from resonance excitation would manifest itself as a current loss. By accelerating single pulses slowly across the aperture (in buckets of constant area and at constant speed) and recording the RF analogue voltage and circulating current on a chart recorder, resonance scans could be obtained. Figure 7 summarizes the scans that were made:

Curve A	solenoid off
Curve B	solenoid on
Curves C to F	solenoid on with vertical bumps to change the beam position in the end-plates
Curve G	solenoid on, all bumps suppressed so that the effect of a 10.27 A beam in ring 1 could be seen.

All curves in Fig. 7 have an initial current of  $\sim 150$  mA but in order to render them more legible, some zero shifts have been introduced. The quantitative results are given in Table 4 where the losses on the resonances are given as a percentage of the initial current.

On the reference scan (curve A - solenoid off), only the 5th order resonances are visible and only 5.7 % of the intensity is lost when crossing the whole family. Once the solenoid is switched on, the losses

Table 4. Current Losses in Resonance Scans.

	$Q_h$	$Q_v$	Resonances in scan order	Current Losses during resonance scans as % of initial current (Fig. )						
				A	B	C	D	E	F	G
1	8.795	8.773	Unidentified	-	-	-	-	-	-	0.5
2	8.799	8.776	$5Q_h = 44$	0.9	11.0	11.2	16.3	9.0	11.7	1.6
3	8.804	8.731	$4Q_h + Q_v = 44$	2.8	15.7	10.4	20.0	11.4	11.2	13.0
4	8.809	8.735	$3Q_h + 2Q_v = 44$	1.4	1.9	1.6	1.7	1.6	2.4	3.0
5	8.814	8.790	$2Q_h + 3Q_v = 44$	0.6	0.5	0.3	0.3	0.1	0.2	0.5
6	8.822	8.797	$Q_h + 4Q_v = 44$	-	-	-	-	-	-	0.9
7	8.826	8.800	$5Q_v = 44$	-	-	-	-	-	-	7.4
8	8.832	8.805	$6Q_h = 53$	-	-	-	-	-	-	0.7
9	8.841	8.814	$9Q_h + 3Q_v = 106$	-	-	-	-	-	-	0.5
10	8.843	8.816	$4Q_h + 2Q_v = 53$	-	-	-	-	-	-	1.9
11	8.846	8.819	$3Q_h + 3Q_v = 53$	-	-	-	-	-	-	3.3
12	8.853	8.829	$Q_h + 5Q_v = 53$	-	-	-	-	-	-	0.2
13	8.862	8.833	$6Q_v = 53$	-	-	-	-	-	-	3.0
14	8.867	8.837	$5Q_h + 2Q_v = 62$	-	-	-	-	-	-	0.5
15	8.883	8.852	$Q_h + 6Q_v = 62$	-	-	-	-	-	-	0.4
16	8.886	8.855	8th order ?	-	-	-	-	-	-	1.4
17	8.890	8.858	$7Q_v = 62$	-	-	-	-	-	-	negligible

Scan A — Solenoid off.

Scan B — Solenoid on, no bump in I1, estimated beam posn. in slot = -1mm\*

Scan C — Solenoid on, -5mm bump I1, estimated beam posn. in slot = -6mm

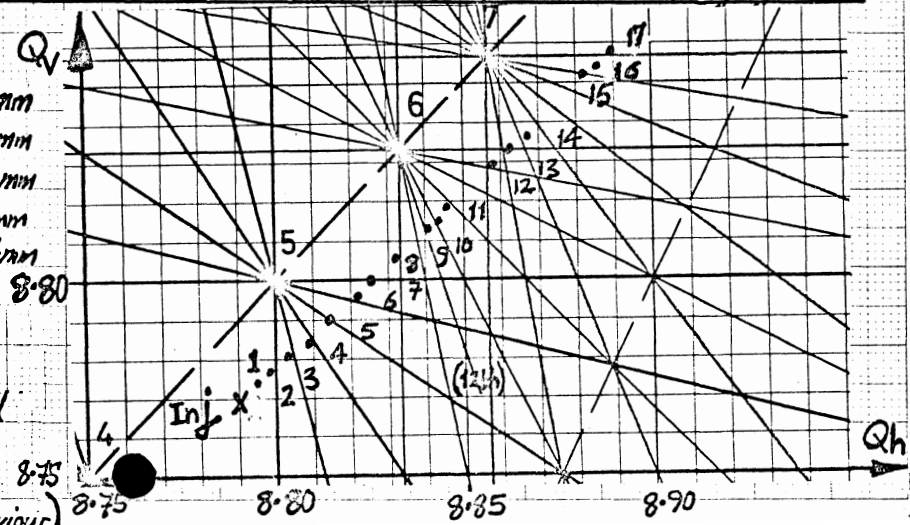
Scan D — Solenoid on, +5mm bump I1, estimated beam posn. in slot = +4mm

Scan E — Solenoid on, +10mm bump I1, estimated beam posn. in slot = +9mm

Scan F — Solenoid on, +15mm bump I1, estimated beam posn. in slot = +14mm

Scan G — Solenoid on, no bump in I1, 10.27A in other ring (R1) 8.80

(\*The vert. beam posn. was calculated by extrapolating from the nearby pickups to the Xn. using the appropriate transfer matrices and assuming no field errors existed in that region. The results show the beam's median plane is curved and the tilt is large at +40mm, At inj.  $Z_v = -1.6mm$ , At  $Z_v = -1.0mm$ , At +40mm  $Z_v = -4.0mm$  - typical ELSA behaviour)



on the 5th order resonances increase to between 22.1 % and 38.3 % according to the conditions. However, the same 5th order resonances are still the only ones that are visible. The variation in the total loss does not correlate well with the beam position in the end-plate slots. Finally, the effect of a beam in the other ring is to excite a wide range of higher order resonances. The total beam lost is still only 38.1 % which can be explained by the fortuitous fact that the beam-beam effect partially compensates the effect of the solenoid on the 5th order resonances (the loss dropping to 18.1 %).

In conclusion, it appears that the solenoid increases the excitation of 5th order resonances by  $\sim 5$  compared to basic machine excitation, but it does not affect higher order resonances which is fortunate when considering the importance of background in stacks. The 5th order resonance excitation is comparable in magnitude with the effect on a beam in the other ring, but the beam-beam effect is able to excite far higher orders as well. The solenoid may, therefore, have a small effect when stacking across the 5th order resonances.

## 9. First impression of the solenoid from a physics point of view

### 9.1 MD run 776

The induced radioactivity in the bicone vacuum chamber was monitored by the scintillation counters A (see Appendix A).

The counting rates measured were:

- before the first injection	: 19.5 K s <sup>-1</sup>	} solenoid at 15 % of 1.5 T
- just after the injection	: $\sim 100$ K s <sup>-1</sup>	
- five minutes later	: 20 K s <sup>-1</sup>	
- just after the first injection:	83 K s <sup>-1</sup>	} solenoid at 1.5 T
- ten minutes later	: 20 K s <sup>-1</sup>	
- twenty minutes later	: 17 K s <sup>-1</sup>	

The induced radioactivity in the bicone vacuum chamber of II was not affected by injection.

## 9.2 Physics run 791

The evolution of the physics conditions in I1 were recorded. Table 5 shows the luminosities, counting rates and backgrounds. The luminosity calibration was made in I1 at the end of run 794 (see Section 9.3).

As a reference, a comparison has been made with previous and similar physics runs without the solenoid:

### 29.11.1976 - Run 782 - 26 GeV/c

I1 = 21.17 A, I2 = 20.18 A,  $\Sigma A$  counters =  $0.85 \times 10^6$  counts.s<sup>-1</sup>  
Backgrounds: Ring 1 = 48 counts.s<sup>-1</sup>, Ring 2 = 181 counts.s<sup>-1</sup>  
BB counts (physics monitors) = 150 s<sup>-1</sup>.

### 4.12.1976 - Run 786 - 26 GeV/c

I1 = 15.29 A, I2 = 20.69 A,  $\Sigma A$  counters =  $0.80 \times 10^6$  counts.s<sup>-1</sup>  
Backgrounds: Ring 1 = 31 counts.s<sup>-1</sup>, Ring 2 = 239 counts.s<sup>-1</sup>  
BB counts = 146 s<sup>-1</sup>.

No noticeable differences in I1 can be seen between physics runs with and without the axial field.

## 9.3 Physics run 794

At the end of the run, a luminosity calibration with 0.5 mm increments (see Fig. 8) was made in I1 using the physics monitors. The value of the effective height obtained was 4.8 mm and the luminosity was  $1.26 \times 10^{31}$  cm<sup>-2</sup>s<sup>-1</sup>. The average of I2, I4 and I5 luminosity measurements gave  $1.25 \times 10^{31}$  cm<sup>-2</sup>s<sup>-1</sup>.

## 9.4 Effect of the solenoid on the cylindrical drift chambers of R108

Figure 9 shows printouts from an on-line, track-reconstruction program. The upper part of the figure shows straight tracks with no analysing field and the lower part of the figure shows curved tracks with the analysing field.

P.J. Bryant  
G. Guignard  
G. Kantardjian  
K. Potter

TABLE 5  
Physics conditions in the solenoid

Time	I1 (A)	I2 (A)	L $\times 10^{31} \text{cm}^{-2} \text{s}^{-1}$	$h_{\text{eff}}$ (mm)	$\Sigma A$ counters $\times 10^6 \text{ counts} \cdot \text{s}^{-1}$	Backgrounds $\text{counts} \cdot \text{s}^{-1}$		Comments
						Ring 1	Ring 2	
Dec. 13 - 20.00 h	22.98	22.41	1.23	4.1	1.49	102	202	22.30h clean-up after centring
- 20.40 h	22.98	22.40	1.19	4.3	1.42	112	615	
- 22.40 h	22.97	22.37	1.21	4.3	1.34	49	195	
Dec. 14 - 2.45 h	22.96	22.35	1.10	4.7	1.28	64	573	5.00h clean-up R2 8.30h clean-up R2 10.30h clean-up R2  22.15h clean-up R1, R2
- 6.50 h	22.96	22.33	1.12	4.6	1.23	66	630	
- 8.40 h	22.96	22.31	1.05	4.9	1.24	70	297	
- 10.40 h	22.96	22.25	1.03	5.0	1.15	107	544	
- 17.00 h	22.94	22.22	0.98	5.2	1.14	176	887	
- 21.00 h	22.94	22.22	0.94	5.4	1.15	235	1163	
- 22.30 h	22.94	22.22	0.93	5.5	1.09	83	295	

References

- 1) Internal Note ISR-MA/PJB/rh dated 28 May 1973, Adjustments of the Split Field Magnet (SFM) Compensators.
- 2) ISR Performance Report ISR-BOM-ES/afm dated 7 January 1977, Runs 772, 776 and 779.
- 3) L. Smith, Lawrence Berkeley Laboratory, Private communication.
- 4) K. Takikawa, A simple and precise method for measuring the coupling coefficient of a difference resonance, Div. Report CERN ISR-MA/75-34.
- 5) G. Guignard, The general theory of all sum and difference resonances in a three-dimensional magnetic field in a synchrotron, CERN report 76-6.
- 6) P.J. Bryant, Possible skew quadrupole schemes for the ISR, Div. Report CERN ISR-MA/75-51.



APPENDIX A

Description of the counters used in Il and belonging to Experiment R108

(see Fig. 10)

1) Beam-beam counters

Luminosity measurements are carried out by means of four sets of two adjacent scintillation counters. They are located one metre from the axis of the solenoid at  $45^\circ$  in azimuth and  $45^\circ$  in polar angle. The beam-beam interaction rate is given by the coincidence of two sets of counters placed diagonally with respect to the central point of the solenoid:

$$BB = (I,up \times 0,down) \text{ or } (I,down \times 0,up).$$

2) Scintillation counters "A"

32 individual scintillation counters form a cylindrical barrel hodoscope around the interaction region which covers a  $2\pi$  azimuthal angle and a  $\pm 56^\circ$  polar angle aperture around the  $90^\circ$  line relative to the ISR. The radius of the hodoscope is 260 mm and each scintillator is 875 mm long, 48 mm wide and 6 mm thick. The sum of the 32 counting rates was monitored.

Remark : The backgrounds were monitored by the standard monitors.

APPENDIX B

Effect of solenoid on the ISR closed orbit

It is perhaps interesting to briefly consider a simplified model of the solenoid comprising a uniform central field terminated by uniform skew gradients inside slots (see Fig. 11.a)). Figures 11.b), c) and d) show how the beam is affected. The central field gives a vertical kick of  $\sim 3.9$  mrad owing to the inclination of the beam with reference to the solenoid's axis. The correction of this kick by a compensator either side of the solenoid causes the beam to cross the end-plates off-axis which creates an estimated  $\pm 0.4$  mm peak-to-peak orbit distortion on the ELSA centre line. Owing to the compensators not being exactly symmetrical about the solenoid, the trajectory inside the solenoid is also slightly asymmetrical and an estimated  $8 \mu\text{rad}$  horizontal kick is imparted to the beam by the central, axial field (see Fig. 11.d)). This adds approximately  $\pm 0.3$  mm peak-to-peak to the closed orbit on ELSA at the centre line. Thus, we have an estimated  $\pm 0.7$  mm peak-to-peak horizontal orbit distortion to be compared to the measured value of 1 mm peak-to-peak.

Although the above is a useful guide, the beam trajectory and the compensator settings have been determined more precisely with a tracking program and a field plot which was supplied by S. Pordes of EP Division. This program makes it possible to quickly calculate for any field-momentum combinations or changes such as the shifted compensator which occurred in the first MD run. It is also possible to follow any given particle through the system. Since two of the low- $\beta$  quadrupoles are positioned between the solenoid and its compensators, the trajectory and compensator settings are different with the low- $\beta$  scheme switched on.

Table 6 summarizes the central orbit trajectories for 26.588 GeV/c and the nominal full field of 1.5 T (2170.1 A) for the low- $\beta$  scheme off which corresponds to the present runs. Since the  $\beta$  and  $\alpha_p$  values are virtually unaffected, the beam size and position can be calculated directly from these figures using the unperturbed machine parameters. A more detailed computer listing from which Table 6 is derived and which includes the field and its derivatives along the trajectory is available.

TABLE 6

Central orbit trajectory through the solenoid and compensators  
for 26.588 GeV/c and the nominal full field of 1.5 T (2170.1 A)  
with the low- $\beta$  scheme off

Element (in beam order)	Distance from intersection* (m)	Displacements from the unperturbed central orbit	
		radial (mm)	vertical (mm)
Entry compensator	-5.76	0.0	0.0
Entry drift space	-5.12	0.0	0.6
Entry solenoid field	-1.60	0.0	6.9
Solenoid	-1.40	0.0	7.3
"	-1.20	0.0	7.6
"	-1.00	0.0	8.0
"	-0.80	0.0	8.3
"	-0.60	0.0	8.6
"	-0.40	0.1	8.7
"	-0.20	0.1	8.8
(Intersection)	0.00	0.1	8.8
"	0.20	0.2	8.7
"	0.40	0.2	8.6
"	0.60	0.2	8.3
"	0.80	0.3	8.0
"	1.00	0.3	7.5
"	1.20	0.3	7.1
"	1.40	0.3	6.7
Entry drift space	1.60	0.3	6.2
Entry compensator	4.07	0.3	0.7
Exit compensator	4.71	0.3**	<0.005

\* negative indicates upstream.

\*\* this distortion propagates around ring; + 0.7 mm peak-to-peak.

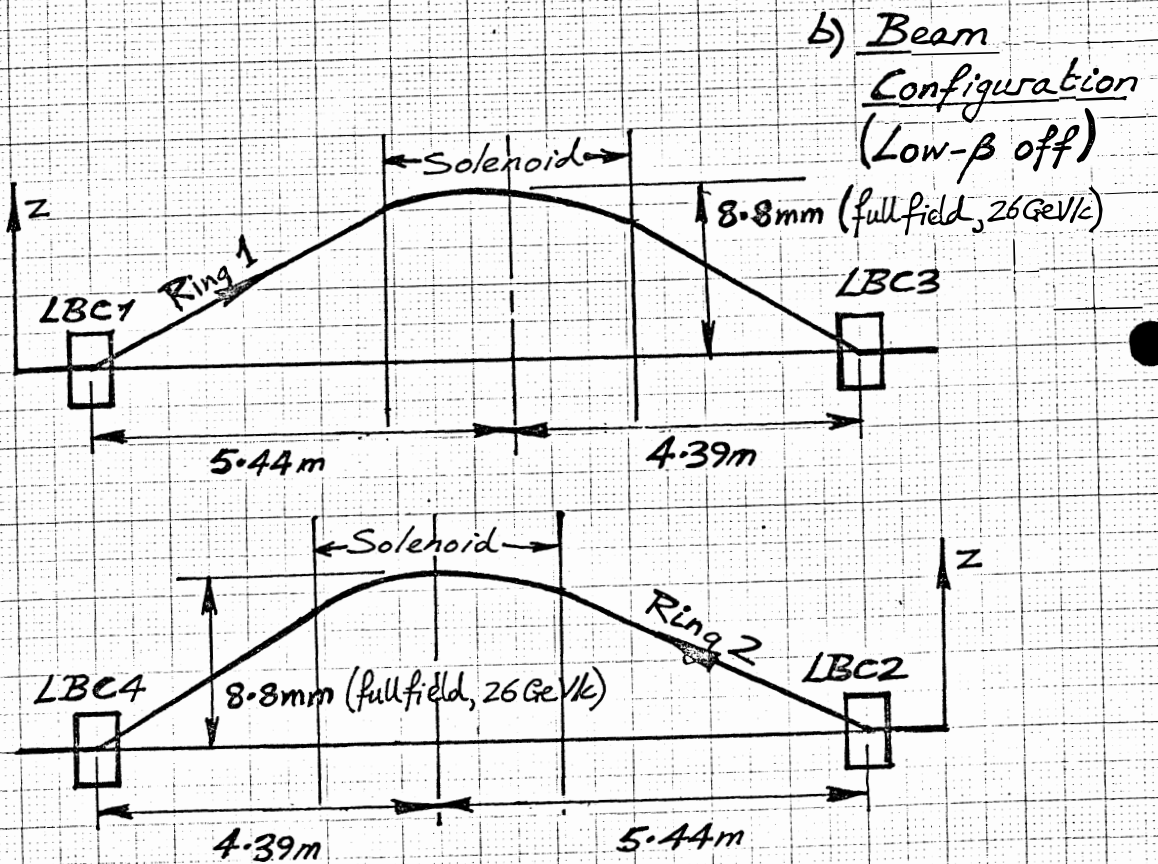
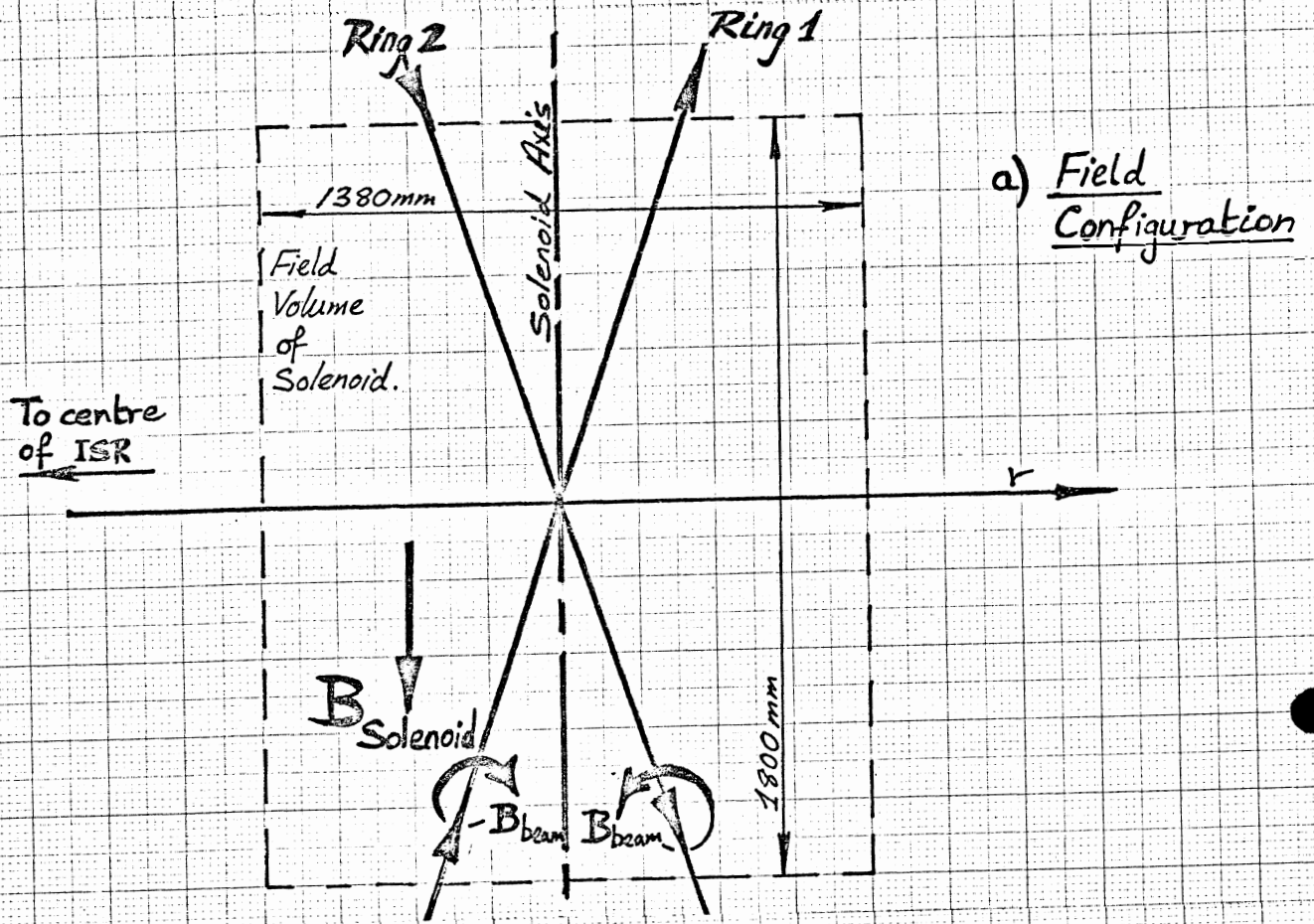


Figure 1. Field and Beam Configurations in I1 Solenoid.

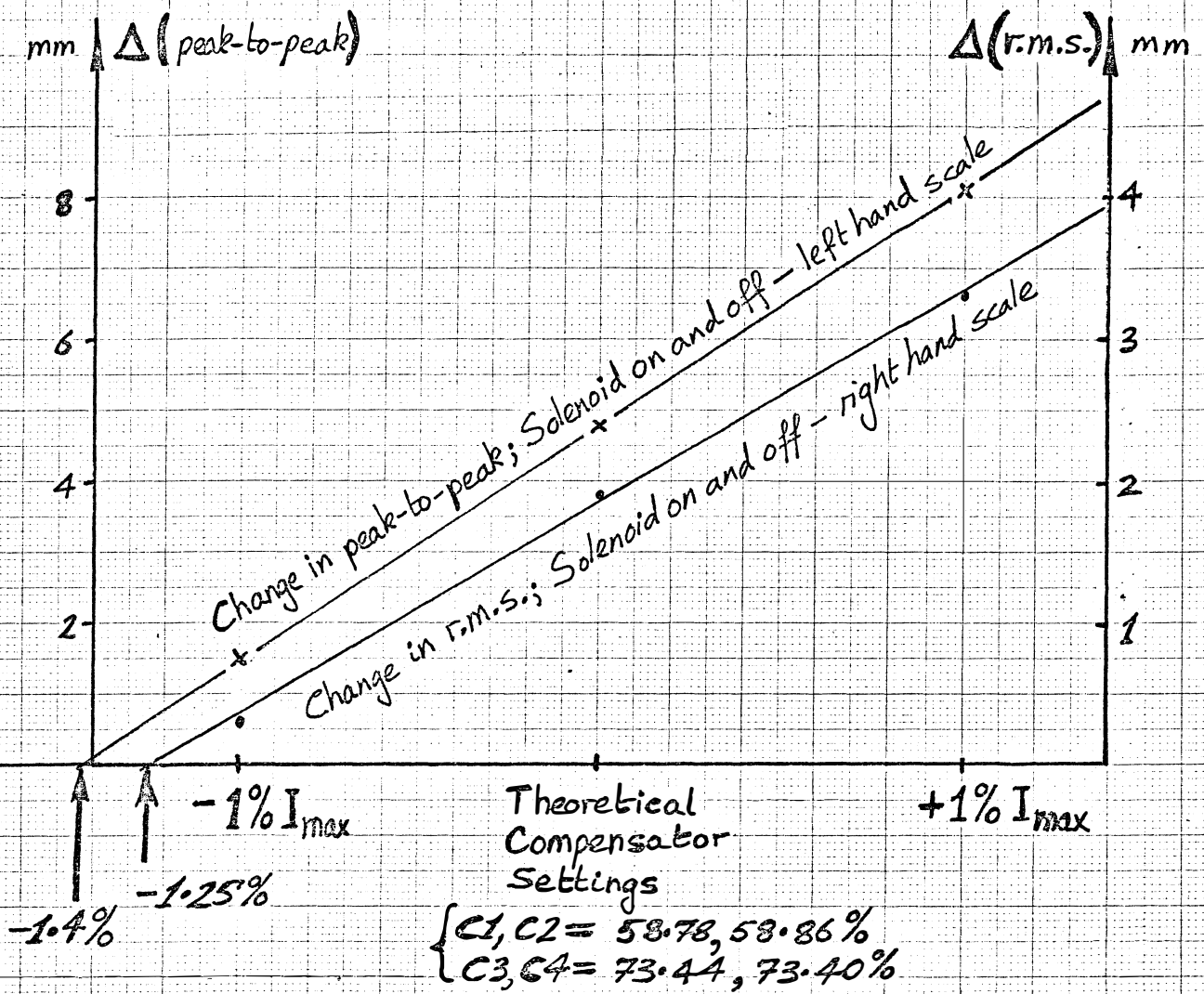
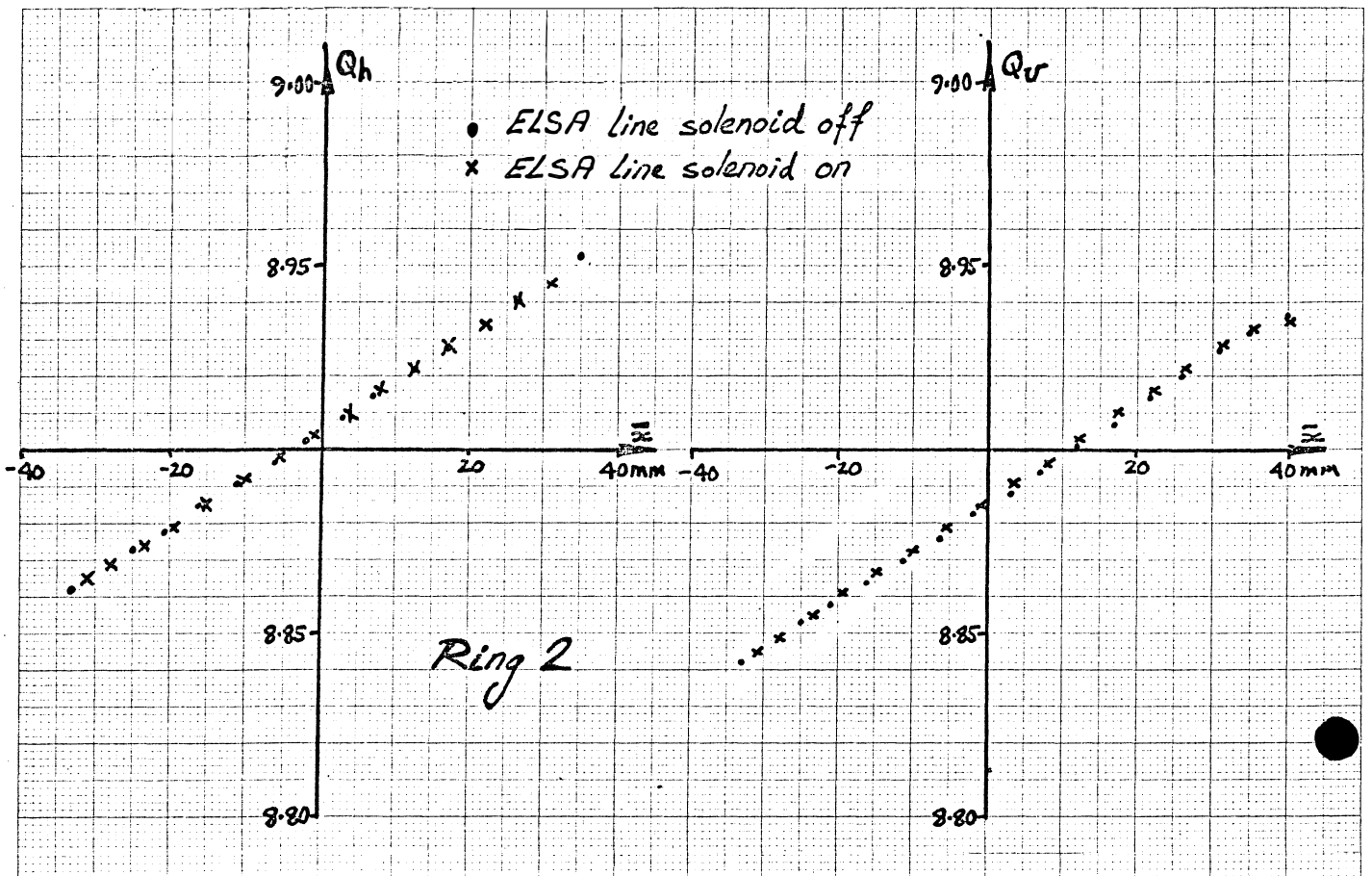


Figure 2. Optimisation of Compensators from Orbit Measurements.



Solenoid off

	BF	R/MM	QH	QV
0	26897	39.72	8.899*	8.937
1	27527	35.35	8.953	8.932
2	28169	31.08	8.644*	8.927
3	28911	26.37	8.941	8.920
4	29688	21.69	8.588*	8.914
5	30497	17.06	8.928	8.907
6	31364	12.36	8.922	8.901
7	32344	7.34	8.915	8.894
8	33296	2.73	8.909	8.888
9	34364	-2.14	8.903	8.882
10	35333	-6.31	8.897	8.876
11	36562	-11.30	8.891	8.870
12	37792	-15.98	8.885	8.864
13	39070	-20.54	8.878	8.858
14	40423	-25.06	8.873	8.853
15	41767	-29.28	8.603*	8.847
16	42951	-32.78	8.864	8.842

Solenoid on.

	BF	R/MM	QH	QV
0	26887	39.81	8.886*	8.935
1	27491	35.60	8.902*	8.933
2	28135	31.31	8.945	8.928
3	28874	26.62	8.941	8.922
4	29627	22.06	8.934	8.916
5	30434	17.43	8.928	8.910
6	31322	12.60	8.922	8.903
7	32202	8.06	8.916	8.896
8	33117	3.59	8.910	8.891
9	34114	-1.01	8.904	8.885
10	35142	-5.50	8.898	8.879
11	36238	-10.00	8.892	8.873
12	37474	-14.78	8.885	8.867
13	38747	-19.40	8.879	8.861
14	39989	-23.63	8.874	8.855
15	41404	-28.15	8.869	8.849
16	42368	-31.06	8.865	8.845

\* Faulty Readings

Figure 3 . ELSA Working Line with I1 Solenoid on and off.

Calibration of Q2  
 at 100% and 26 GeV/c  
 calculated 0.2485  
 measured 0.24

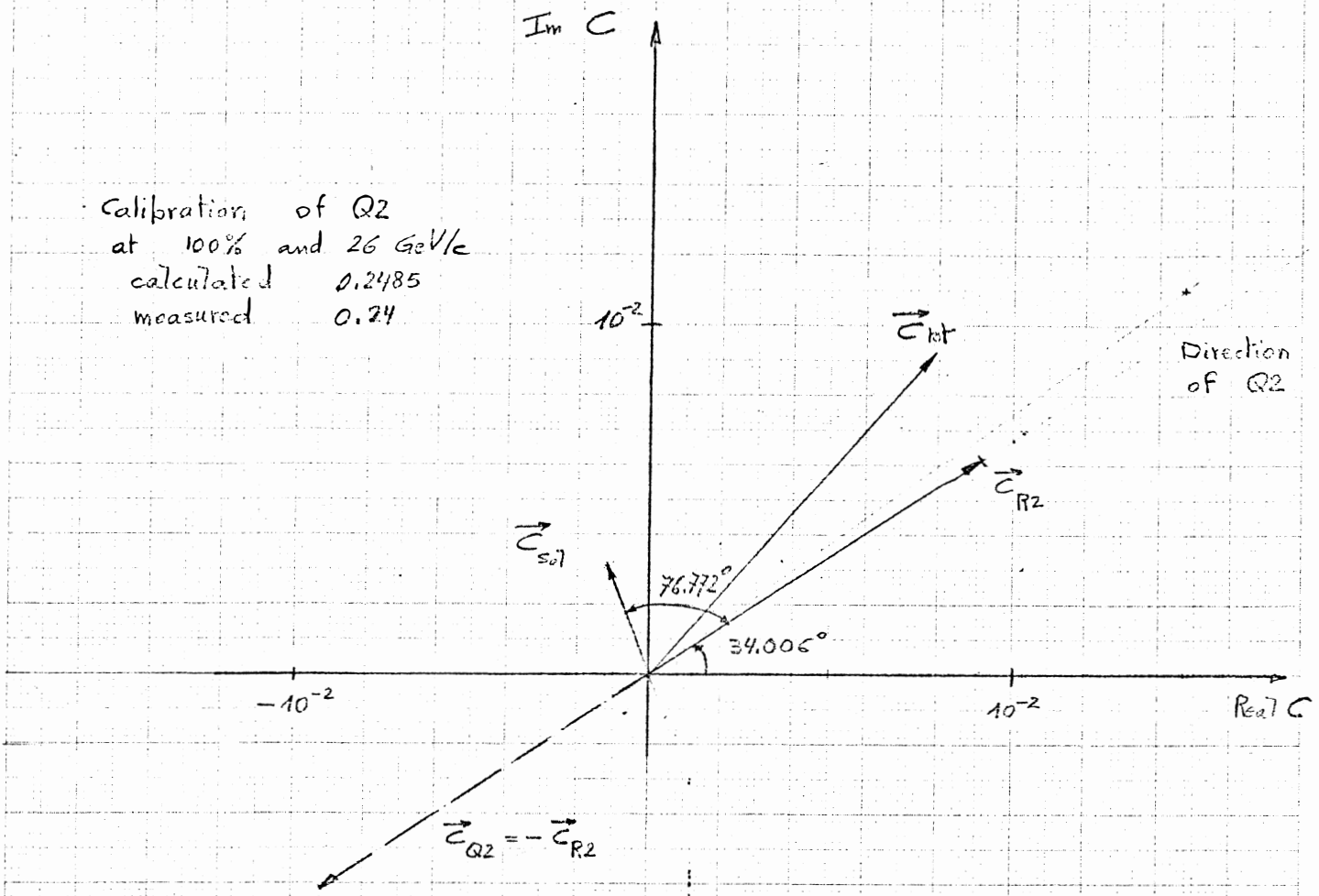


Fig. 4 Residual coupling in R2 and solenoid coupling

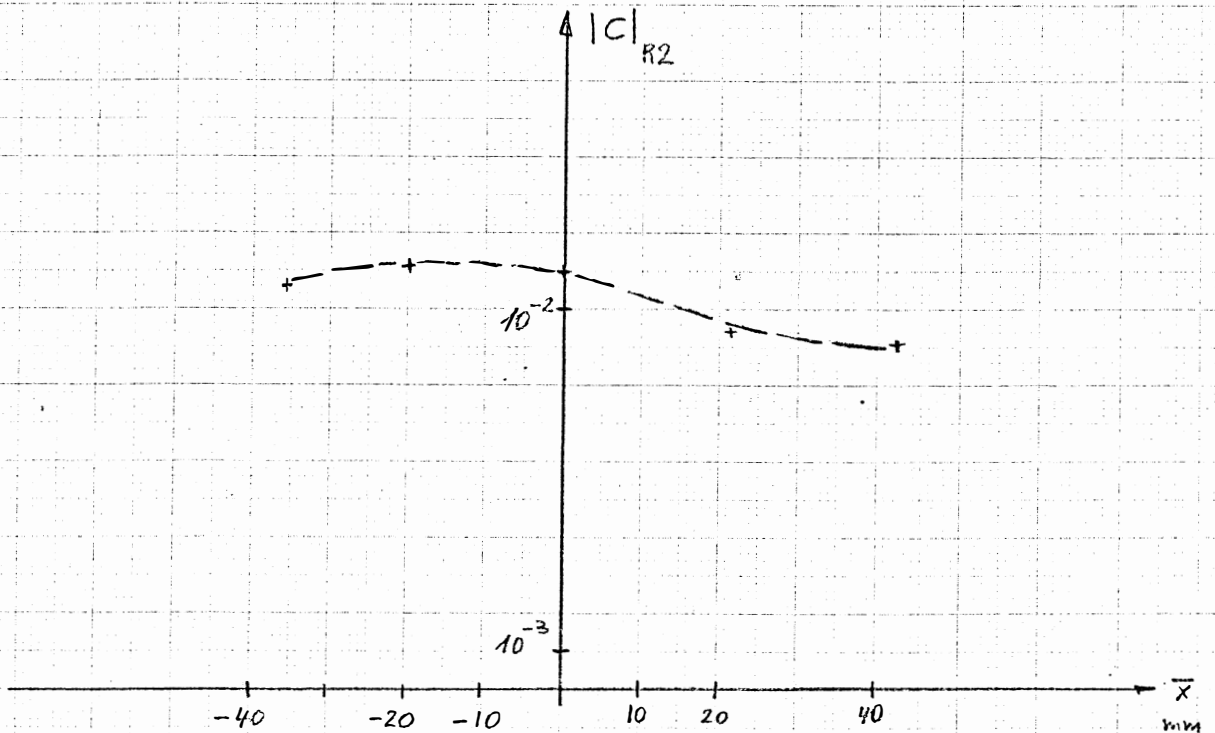
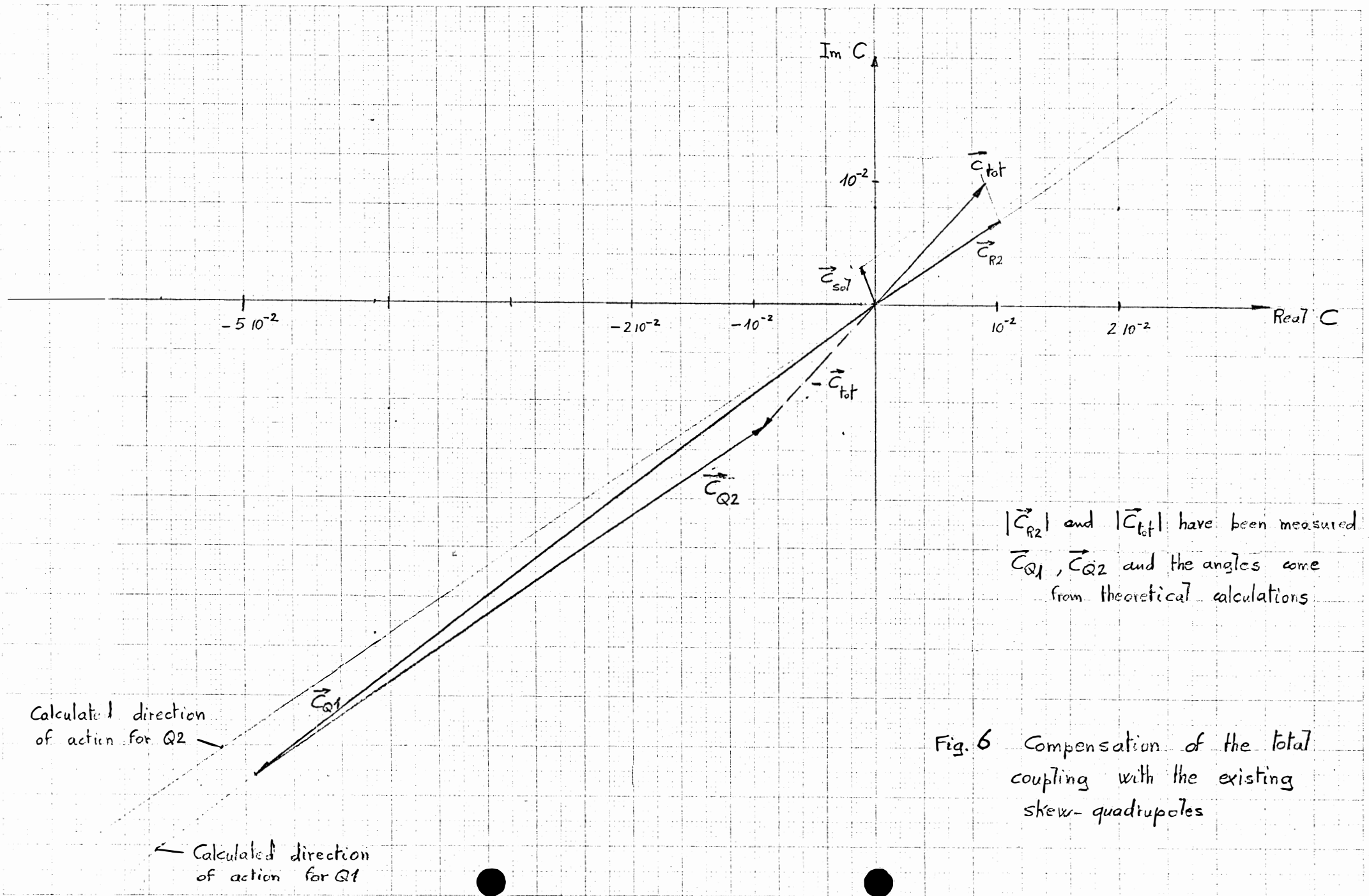


Fig. 5 Variation of the coupling in R2 on EL26 with the radial position



$|\vec{C}_{R2}|$  and  $|\vec{C}_{tot}|$  have been measured  
 $\vec{C}_{Q1}$ ,  $\vec{C}_{Q2}$  and the angles come  
 from theoretical calculations

Fig. 6 Compensation of the total  
 coupling with the existing  
 skew-quadrupoles



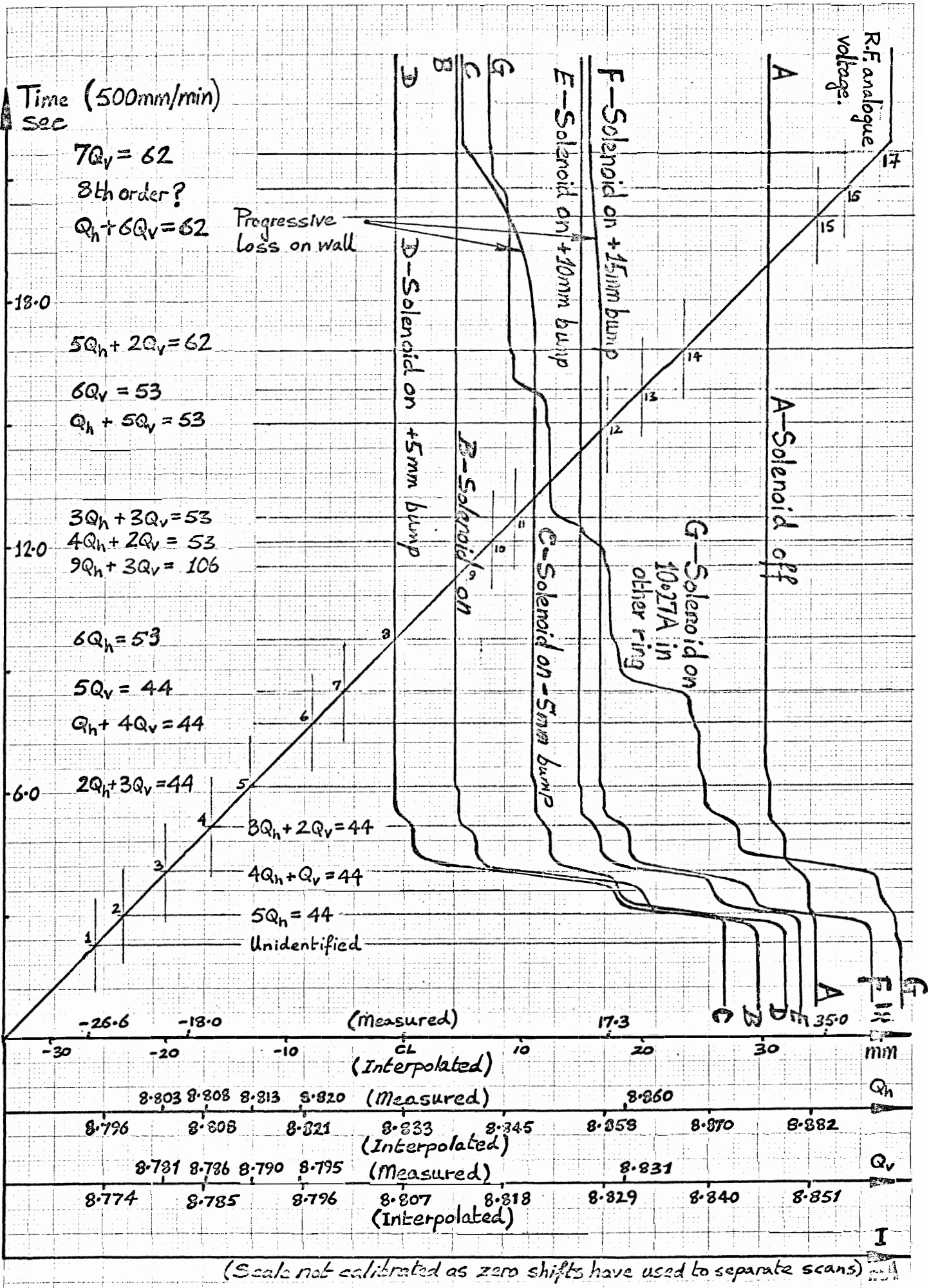


Figure 7. Resonance Scans. (Quantitative results in Table 4)

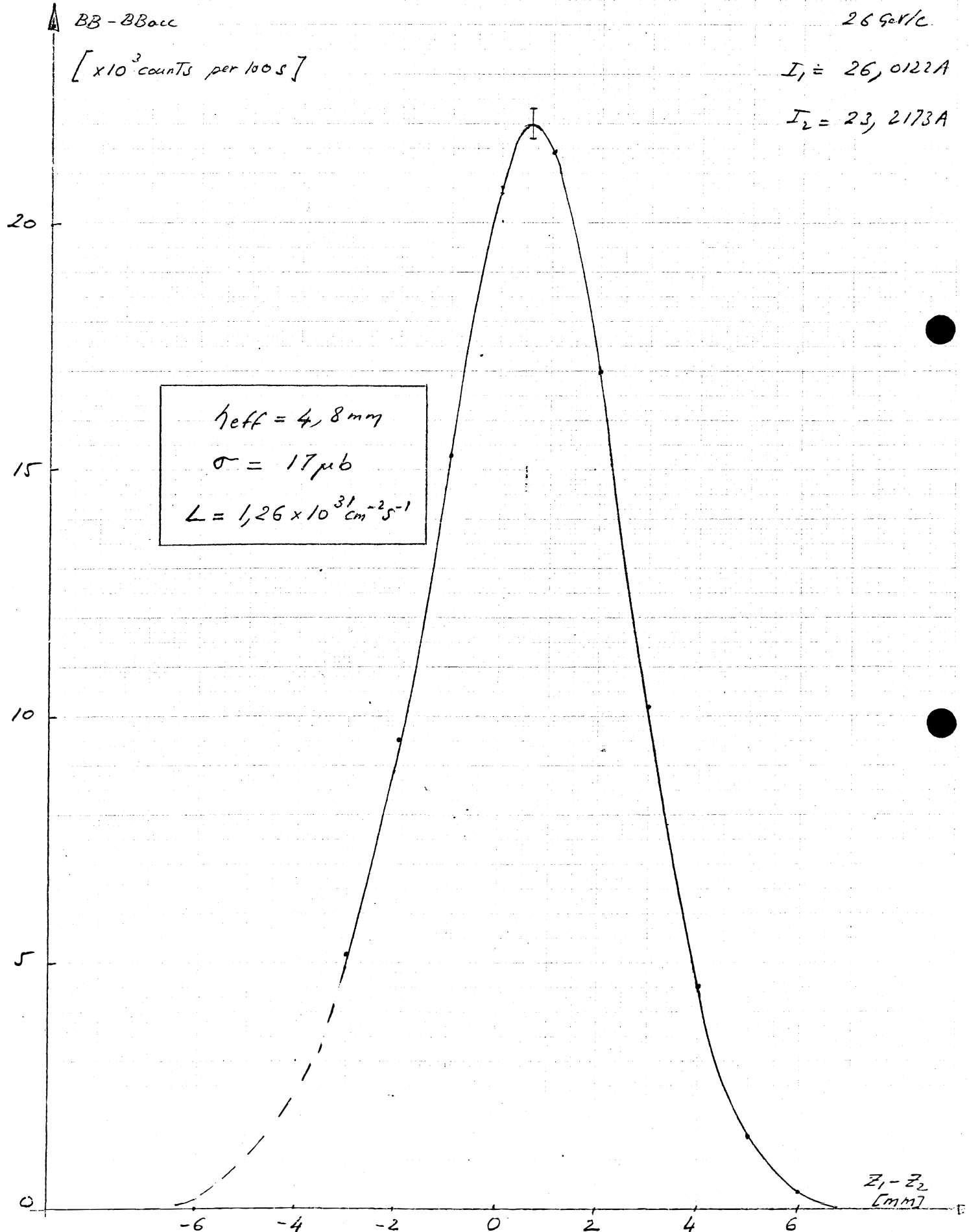
Figure 8. Luminosity calibration curve obtained  
in Intersection 1  
using the physics monitors

Run 794

26901/c

$I_1 = 26,0122A$

$I_2 = 23,2173A$



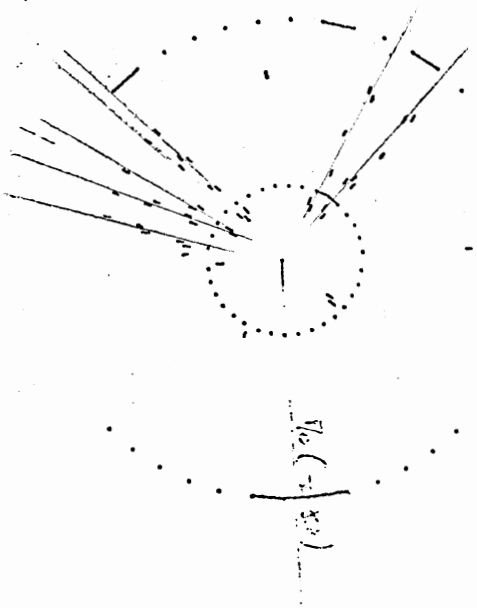
EVENT 185 ENERGY 5.4 .0

TRIGGER GI

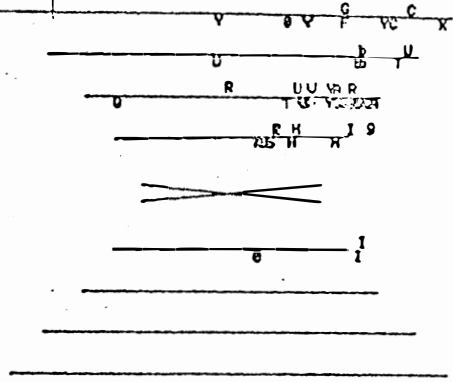
.0 .0 .0 .0 .0 .0 .0 .0 .0 .0 .0 .0

[Empty box]

27-11-7



SOLENOID off



.0 .0 .0 .0 .0 .0 5.0 .0 .3 .0 .0 .0

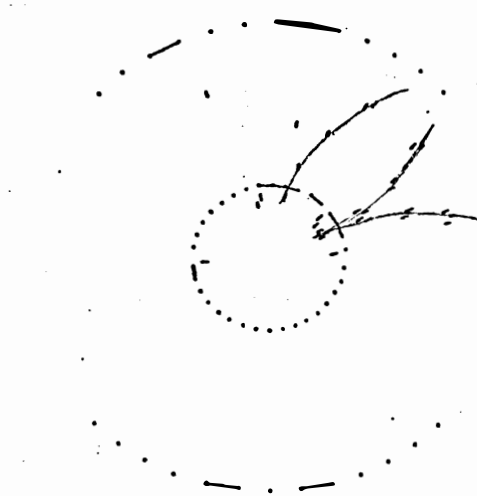
.3  
5.0

14-12-76  
Run 791

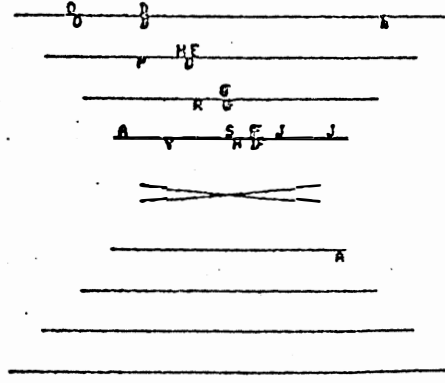
RUN 1982 EVENT 3483 ENERGY 1.1 2.2 HDWARE 7325 2675 TRIGGER PP

.0 .0 1.4 .0 .0 .0 .0 .4 .0 .1 .0 .0

.1  
.4  
1.4



SOLENOID ON



.0 .0 .0 .0 .0 .0 .0 .0 .0 .0 1.0 .0

1.0

Locations from the Cylindrical Drift Chambers.

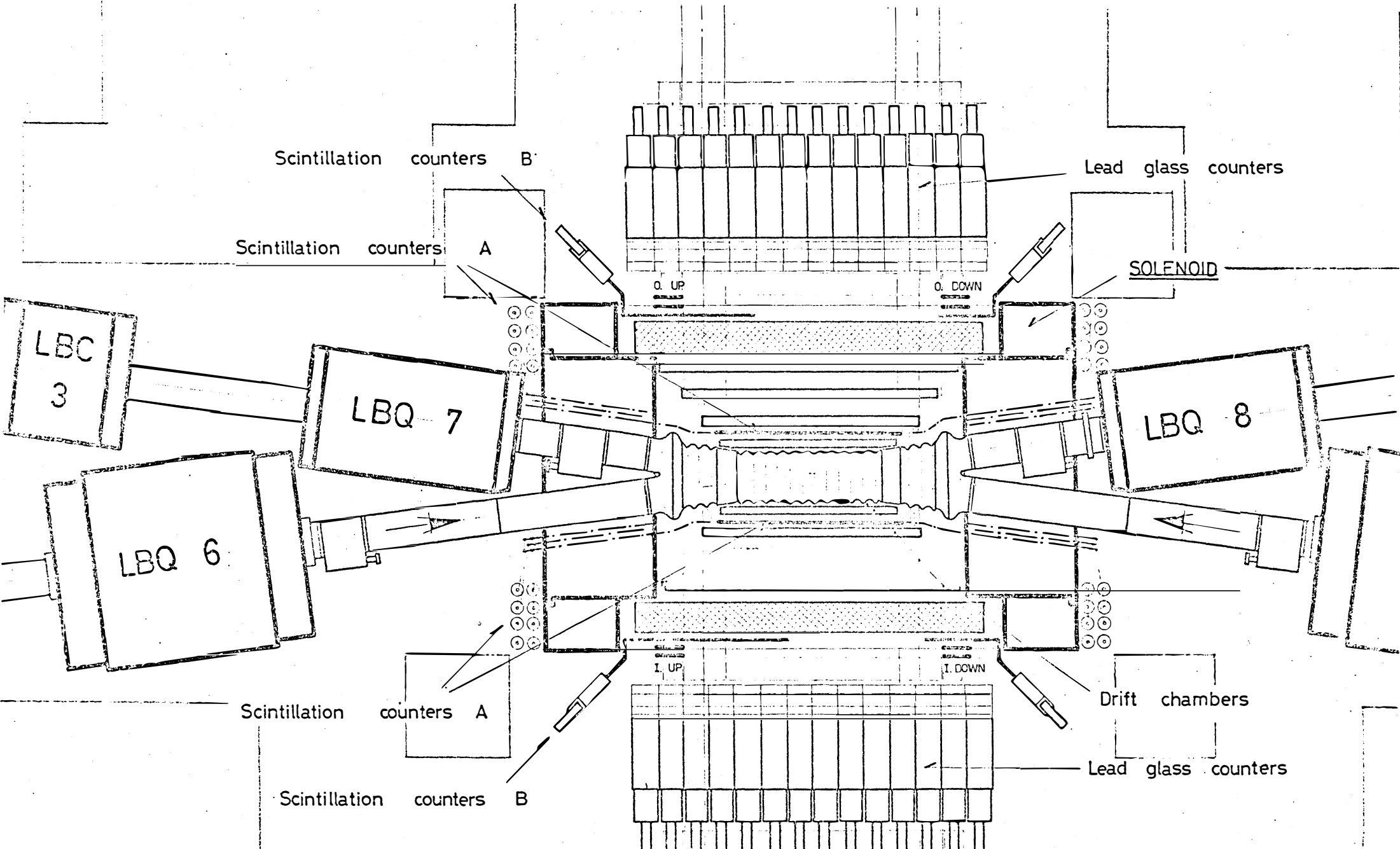
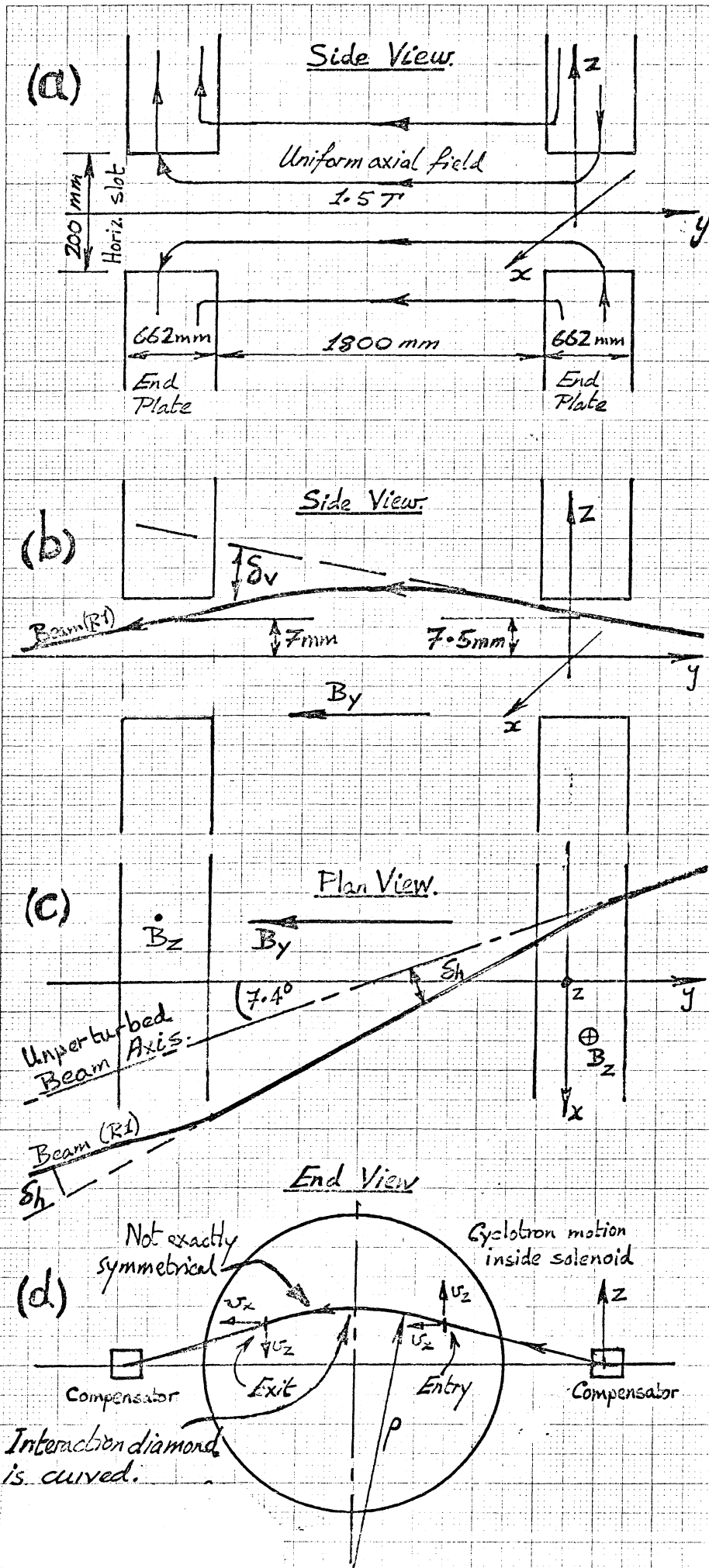


Figure 10. *Layout of Magnets and Counters in I1. (experiment R108)*



Approximate Expressions and Calculations.

Central region:  
 $B_y$  - Uniform 1.5 T axial field.

End Plate: Using Gauss' Theorem,

$B_z = \frac{B_y}{2R} z$   $l =$  thickness of end plate

$\int_{\text{end plate}} \frac{dB_z}{dz} dy = \frac{B_y}{2} = 0.75T$

This skew gradient causes coupling.

Kicks received by beam.

$\delta_v = \frac{B_y L \sin 7.4^\circ}{B_p}$

$L =$  lgh. of central region  
 $B_p =$  magnetic rigidity.

At 26.588 GeV/c,  $\delta_v = 3.9 \text{ mrad}$

- Average beam heights in slots can be estimated from compensator magnets (Fig. 1)

$\delta_h = \frac{h \int \left(\frac{dB_z}{dz}\right) dy}{B_p}$

$h$  is beam poon. in slot.

At 26.588 GeV/c,  $\delta_h = 0.06 \text{ mrad}$

Orbit Distortion.

- Vertically localised by compensator  
 - Horizontally if left uncorrected

$x(\phi) = \sqrt{\beta_x \beta_y} \cdot Z_0 \sin(\Delta\phi) \cdot Z \sin(\pi\phi)$

$\sin Q(\pi + \phi - \psi)$  (for  $\phi < \psi$ )

$\Delta\phi$  is betatron phase advance between end plates,  $\psi$  is phase at centre of solenoid,  $\phi$  is phase at observation point.

At 26 GeV/c  $x_{\text{max}} = \pm 0.4 \text{ mm}$   
 ELSA  $\nabla$

Cyclotron motion in the axial field.

Radius of gyration  $\rho = \frac{Z_p \sin 7.4^\circ}{B_y}$

For 26.588 GeV/c,  $\rho = 7.685 \text{ m}$

Owing to a small asymmetry in the compensators  $v_x(\text{entry})$  (does not quite equal  $v_x(\text{exit})$ ), as a result there is an almost negligible kick of

Figure 11. Approximate Expressions and Calculations Using a Simplified Model of the Solenoid.